A&A 424, 765–772 (2004)
DOI: 10.1051/0004-6361:20041042

Astronomy & Astrophysics

Gamma ray signatures from Galactic neutralino annihilation

G. Valle[1,2,3,⋆]

[1] Dipartimento di Fisica "Enrico Fermi", Università di Pisa, via F. Buonarroti 2, Pisa 56127, Italy
[2] Dipartimento di Fisica, Università di Siena, via Roma 56, Siena 53100, Italy
[3] Istituto Nazionale di Fisica Nucleare, Sezione di Pisa, via F. Buonarroti 2, Pisa 56127, Italy
e-mail: giada.valle@pi.infn.it

Received 6 April 2004 / Accepted 26 May 2004

Abstract. Direct observations of cosmic photon spectra from neutralino annihilation at energies above EGRET data might reveal the presence of weakly interacting massive particle (WIMP) dark matter in the Universe.
Calculations of the rates for the continuum γ channel and γ-ray line are reviewed. Both the continuum γ-ray spectrum and the γ-ray line arising from neutralino annihilation are studied. Flux estimates are inherently model-dependent; they suffer from uncertainties due to the large allowed ranges in supersymmetrical parameter-space and from a variety of astrophysical models of the dark matter halo profiles. Our analysis allows detection predictions for orbital and ground-based experiments. As an application, we investigate the number of signal events expected to be detected in an orbital experiment (AMS-02) and we make a comparison with atmospheric Cerenkov telescopes.

Key words. cosmology: dark matter – cosmology: miscellaneous

1. Introduction

Evidence showing the need for some form of non-luminous but gravitationally influential matter exists on many scales, ranging from galaxies to superclusters of galaxies up to the Gpc scale (see for instance, Hagiwara et al. 2002). On the smallest scale (≃kpc) robust evidence for dark matter (DM) comes from the rotation curves of spiral galaxies, while on cluster and supercluster scales (multi Mpc) compelling evidence arises from gravitational lensing. However, the evidence on the Galactic scale does not permit any inferences about the nature (baryonic or non baryonic) of the DM. On cosmological scales, the cosmic microwave background radiation (CMB) anisotropies, obtained first by COBE and recently by the WMAP satellite shed light on the nature of DM. The favored scenario is a flat cold dark matter Λ dominated Universe (Λ-CDM cosmology) with $\Omega_\Lambda \simeq 0.73$, $\Omega_{\rm baryons} \simeq 0.044$, $\Omega_{\rm luminous} \simeq 0.0035$ and $\Omega_{\rm matter} \simeq 0.27$, indicating that the bulk of matter is dark and is mainly non-baryonic (Spergel et al. 2003; Bennet et al. 2003). The information which we have at present suggests that the bulk of DM particles are stable, cold and weakly interacting. These considerations point to the neutralino χ as a promising DM candidate. It is the lightest particle predicted in the supersymmetric theories with the conservation of the R parity satisfying the previous requirements (Jungman et al. 1996; Ellis 1999).

⋆ Dipartimento di Fisica "Enrico Fermi", Gruppo di Ricerca in Astrofisica, Università di Pisa, via F. Buonarroti 2, Pisa 56127, Italy.

2. Gamma-ray signals

Among the variety of channels for neutralino annihilation, we will concentrate here on a possible indirect signature of dark matter through the production of γ-rays. The photon energy distribution has two types of contributions: resonant line and continuum. The line channel results from direct annihilation $\chi\chi \to \gamma\gamma$ and $\chi\chi \to Z\gamma$. Since the neutralino velocities in the halo are of the order of 10^{-3} c, the annihilation can be considered to occur at rest and the line width is narrow (order $\Delta E_\gamma/E_\gamma \simeq 10^{-3}$). The position of the resonant line for this processe is $E_\gamma = m_\chi$ for the $\gamma\gamma$ channel and $E_\gamma = m_\chi - m_Z^2/4m_\chi$ for the $Z\gamma$ channel ($c = 1$); the energies of the two lines coincide for high values of m_χ. The energy of the photon for $Z\gamma$ line vanishes as m_χ tends to $m_Z/2$. The continuum contribution is due mainly to the decay of secondary π^0 mesons. In contrast to the characteristic signature arising from the line processes, the lack of any distinguishing feature in the continuum spectrum makes it difficult to discriminate it among other possible γ-ray sources. However, this mechanism produces a larger number of photons than the resonant case. Tasitsiomi & Olinto (2002) show that the continuum photon spectrum can be calculated from the π^0 spectrum:

$$\frac{{\rm d}N_{\pi^0}}{{\rm d}x_\pi} \simeq \frac{5}{16} x_\pi^{-3/2}(1-x_\pi)^2, \tag{1}$$

with $x_\pi = E_{\pi^0}/m_\chi$. The continuum photon spectrum can be written as:

$$\frac{{\rm d}N_{\rm cont}}{{\rm d}x_\gamma} \simeq \int_{x_\gamma}^1 \frac{2}{x_\pi}\frac{{\rm d}N_{\pi^0}}{{\rm d}x_\pi}\,{\rm d}x_\pi \tag{2}$$

with $x_\gamma = E_\gamma/m_\chi$.

The γ-ray intensity from neutralino annihilation is:

$$I_\gamma(\xi) = \frac{N_\gamma \langle \sigma \mathrm{v} \rangle}{4\pi m_\chi^2} \int_0^\infty \rho_\chi^2(L)\, \mathrm{d}L(\xi) \ \ \mathrm{cm}^{-2}\ \mathrm{s}^{-1}\ \mathrm{sr}^{-1}, \tag{3}$$

where ξ is the angle between the direction of the Galactic Center and the line of observation, ρ_χ is the halo dark matter density at distance L along the line of sight, $\langle \sigma \mathrm{v} \rangle$ is the thermally average product of the cross section times the relative velocity, related to supersymmetrical models (hereafter, for simplicity, we will refer to $\langle \sigma \mathrm{v} \rangle$ as the cross section), and N_γ is the number of photons created per annihilation. In the case of $\chi\chi \rightarrow \gamma\gamma$ and $\chi\chi \rightarrow Z\gamma$ the values of N_γ are, respectively, $N_\gamma = 2$ and $N_\gamma = 1$. For the continuum N_γ is the number of photons integrated above the detection threshold E_{th}. With the π^0 spectrum in Eq. (1), integrating Eq. (2), we obtain:

$$\begin{aligned} N_\gamma\,(E \geq E_{\mathrm{th}}) \ &= \ \int_{x_{\mathrm{th}}}^1 \frac{\mathrm{d}N_\gamma}{\mathrm{d}x_\gamma}\, \mathrm{d}x_\gamma \\ &= \ \frac{5}{6} x_{\mathrm{th}}^{3/2} - \frac{10}{3} x_{\mathrm{th}} + 5 x_{\mathrm{th}}^{1/2} + \frac{5}{6} x_{\mathrm{th}}^{-1/2} - \frac{10}{3}, \end{aligned} \tag{4}$$

where $x_{\mathrm{th}} = E_{\mathrm{th}}/m_\chi$. The intensity of Eq. (3) can be written as the product of one part, S, depending on the SUSY parameters and decay model, and one part related to a specific astrophysical model of the halo dark matter profile:

$$I_\gamma(\xi) = S\ \frac{\rho_0^2 R_0}{4\pi} J(\xi)\ \mathrm{cm}^{-2}\ \mathrm{s}^{-1}\ \mathrm{sr}^{-1}, \tag{5}$$

where:

$$S = \frac{N_\gamma \langle \sigma \mathrm{v} \rangle}{m_\chi^2}\ \mathrm{cm}^3\ \mathrm{s}^{-1}\ \mathrm{GeV}^{-2}, \tag{6}$$

and $J(\xi)$ is a dimensionless function (e.g. Bergstrom et al. 2001):

$$J(\xi) \equiv \int_0^\infty \frac{\rho_\chi^2}{R_0\, \rho_0^2}\, \mathrm{d}L(\xi), \tag{7}$$

where R_0 is the solar Galactocentric distance and ρ_0 is the solar neighborhood dark matter halo mass density.

3. Dark matter halo profiles

In CDM cosmologies dark matter halos form hierarchically; smaller halos form first from initial density fluctuations and they merge to become larger halos (Fukushige & Makino 2000). Various N-body simulations of hierarchical CDM clustering have been performed in recent years (e.g. Steinmetz & Navarro 2002).

The general parametrization of spherically symmetric dark matter halo profiles is given by:

$$\rho(r) = \rho_a \left(\frac{r}{a}\right)^{-\gamma} \left[1 + \left(\frac{r}{a}\right)^{\alpha}\right]^{\frac{\gamma-\beta}{\alpha}} \tag{8}$$

where a is the scale radius, r is the distance from the Galactic Center (Zhao 1996; Kravtsov et al. 1997). The relationship between the distance L along the line of sight, the distance from the Galactic Center r, the viewing angle ξ and R_0 is given by:

$$r^2 = L^2 + R_0^2 - 2LR_0 \cos\xi.$$

Table 1. Dark matter halo profiles. The parameters are taken from Dehnen & Binney (1998) and Bergstrom et al. (1998).

Model	(α, β, γ)	R_0 (kpc)	a (kpc)	ρ_a ($M_\odot$/pc^3)	ρ_0 (GeV/cm^3)
NFW	1, 3, 1	8.0	21.8	0.006159	0.34
D&B 2d					
NFW	1, 3, 1	8.0	5.236	0.1101	0.43
D&B 4d					
Moore	1.5, 3, 1.5	8.5	33.2	0.001640	0.4
S_{p}	2, 2, 0	8.5	4.0	0.04555	0.3
K_{b}	2, 3, 0.4	8.5	12.0	0.01627	0.4

Navarro, Frenk and White (hereafter NFW) (Navarro et al. 1996) performed N-body simulation of halo formation and found that the profile of dark matter halos can be fitted by the universal form:

$$\rho(r) = \frac{\rho_a}{\frac{r}{a}\left[1 + (\frac{r}{a})^2\right]}, \tag{9}$$

i.e. they obtained a cuspy profile, characterized by (α, β, γ) = (1, 3, 1). They also found that the profile is independent of the halo mass, the initial density fluctuation spectrum, and the values of the cosmological parameters. A coreless profile with a mild singularity toward the Galactic Center with $\gamma \simeq 0.2$–0.4 was proposed by Kravtsov et al. (1997). Both results disagree with the modified isothermal distribution, (α, β, γ) = (2, 2, 0) (hereafter S_{p} profile), which is nonsingular with a core radius of $\simeq a$ constant for $r \ll a$, and falls off as r^{-2} for $r \gg a$. Recently, Moore et al. (1999, 2000) performed simulations with $\gtrsim 10^6$ particles and found that halos have a cusp that is steeper than the NFW profile; they proposed a universal modified profile $(\alpha, \beta, \gamma) = (1.5, 3, 1.5)$. Jing & Suto (2000) performed a series of N-body simulations and concluded instead that the power of the cusp depends on mass, varying from –1.5 for a galaxy-mass halo, to –1.1 for a cluster-mass halo.

Turning to the Milky Way, although the orbital motions of the satellites of the Galaxy indicate the presence of a nonluminous matter component, it is not possible at present to discriminate between the different radial dark matter halo profiles reported in the literature. In fact, the mass distribution of the Galaxy and the relative importance of its various components (bulge, disk and halo) are not well constrained by the available observational data (Dehnen & Binney 1998).

It is worth noting that even within a specific halo profile, the predicted γ flux depends on three parameters: the normalization constant of the halo profile (chosen as the value of the halo density ρ_0 at our Galactocentric distance R_0), the length scale a, and R_0. After choosing the functional form for the halo profile, it is possible to determine the allowed regions in the parameter space. An extensive analysis can be found in Bergstrom et al. (1998). We will concentrate our analysis on the halo profiles listed in Table 1, where (α, β, γ), a (kpc), ρ_a, are the parameters in Eq. (8).

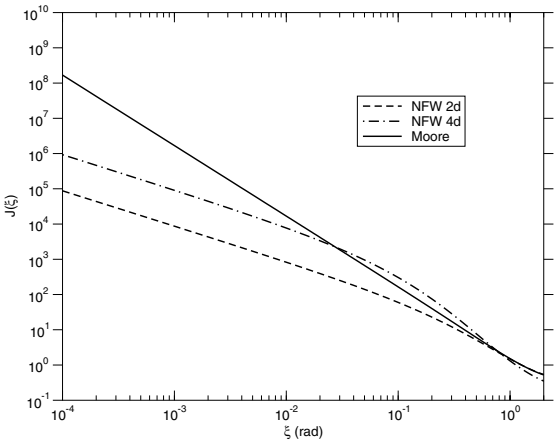

Fig. 1. Function $J(\xi)$ as defined in Eq. (7) for the halo profiles NFW (D&B 2d), NFW (D&B 4d), Moore et al. in Table 1.

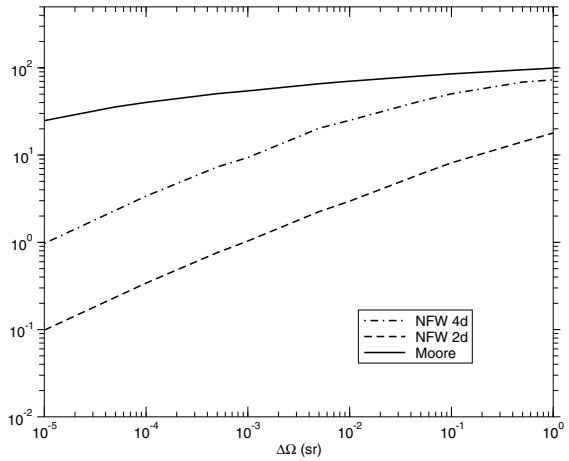

Fig. 2. $\int_{\Delta\Omega} J(\xi)\ \mathrm{d}\Omega$ as a function of $\Delta\Omega$ for halo profiles NFW (D&B 2d), NFW (D&B 4d) and Moore et al. in Table 1.

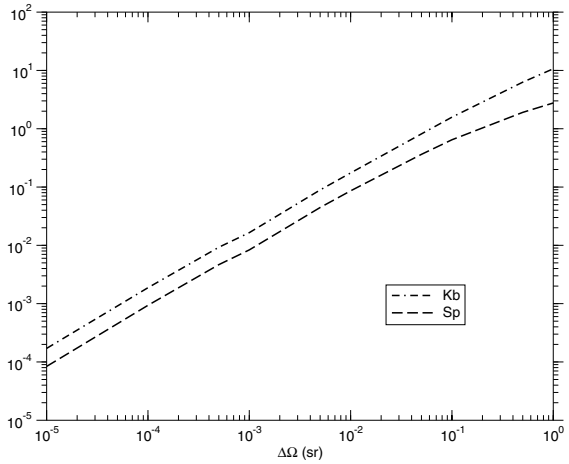

Fig. 3. $\int_{\Delta\Omega} J(\xi)\ \mathrm{d}\Omega$ as a function of $\Delta\Omega$ for halo profiles S_p and K_b, in Table 1.

4. Rate estimates

To derive a flux for a specific angular acceptance, we integrate Eq. (5) over $\Delta\Omega$, obtaining:

$$F_\gamma(\xi;\Delta\Omega) = S\ \frac{\rho_0^2 R_0}{4\pi} \int_{\Delta\Omega} J(\xi)\ \mathrm{d}\Omega\ \ \mathrm{cm}^{-2}\,\mathrm{s}^{-1}. \qquad (10)$$

The photon flux from neutralino annihilation in the Galactic halo strongly depends on the neutralino radial distribution; since the intensity is proportional to ρ_χ^2 (see Eq. (3)) any enhancement of the density results in a sharp increase in the photon flux. Such enhancement is provided by dark matter halo profiles that are peaked toward the Galactic Center, such as the Moore et al. profile.

To obtain an idea of the uncertainties for the γ-production as a function of $\rho(r)$, Fig. 1 shows the integral of the squared dark matter halo density along the line of sight, i.e. the dependence of $J(\xi)$ vs. the angle ξ. Figures 2 and 3 show the dependence of the integration of this quantity over the solid angle $\Delta\Omega$ around the Galactic Center, i.e. $J(\xi;\Delta\Omega) \equiv \int_{\Delta\Omega} J(\xi)\ \mathrm{d}\Omega$ as a function of $\Delta\Omega$. The function $J(\xi)$ is highly variable at small ξ, especially for the cuspy profiles such as Moore's.

The integral $J(\xi;\Delta\Omega)$ was calculated with an adaptive Monte Carlo technique, using the MISER algorithm (Press & Farrar 1990) with a sufficient number of points to achieve a precision of 0.1% or better. The density profiles are valid to within 0.01 pc of the core of Sgr A*, a black hole with $M \simeq 3\times10^6\ M_\odot$ (Schoedel et al. 2004).

5. The gamma background

To evaluate the neutralino signature in the gamma spectrum, the irreducible γ background, consisting of galactic and extragalactic components, must be estimated.

After removing the contribution from resolved point sources and the Galactic diffuse emission, the isotropic extragalactic emission is well described by a power law photon spectrum (Sreekumar et al. 1998):

$$\frac{\mathrm{d}N_\mathrm{extragal}}{\mathrm{d}E} = k\left(\frac{E}{0.451\ \mathrm{GeV}}\right)^{-\beta}\ \mathrm{cm}^{-2}\,\mathrm{s}^{-1}\,\mathrm{sr}^{-1}\,\mathrm{GeV}^{-1}, \qquad (11)$$

where $k = (7.32 \pm 0.34)\times10^{-6}$ and $\beta = (2.10 \pm 0.03)$. The Galactic γ background is mainly due to protons and electrons from cosmic rays that interact with the interstellar medium. The dominant component of the γ-ray spectrum above 1 GeV is due to π^0 decay, the γ-ray spectral index of which asymptotically approaches the cosmic ray spectral index. The spatial distribution of the diffuse emission has been determined after removing the contribution from point sources detected with greater than 5σ significance (Hunter et al. 1997).

For the diffuse γ-ray emission we assume a power law in energy in the form:

$$\frac{\mathrm{d}N_{bg}}{\mathrm{d}E_\gamma}(E_\gamma,l,b) = N_0(l,b)\left(\frac{E_\gamma}{1\ \mathrm{GeV}}\right)^{-\alpha}\ \mathrm{cm}^{-2}\,\mathrm{s}^{-1}\,\mathrm{sr}^{-1}\,\mathrm{GeV}^{-1}, \qquad (12)$$

where l is the galactic longitude ($-180^\circ \le l \le 180^\circ$), b is the galactic latitude ($-90^\circ \le b \le 90^\circ$). $N_0(l,b)$ is strongly dependent on the sky position. We refer here to Hunter et al. (1997) who show (their Fig. 5) that the deconvolved average Galactic Center flux ($355^\circ \le l \le 5^\circ$ and $-2^\circ \le b \le 2^\circ$) at 1 GeV is $N_0(0,0) \simeq 120\times10^{-6}\ \mathrm{GeV}^{-1}\,\mathrm{cm}^{-2}\,\mathrm{sr}^{-1}\,\mathrm{s}^{-1}$. We assume this value and we adopt $\alpha = 2.7$. The assumed α is supported by the preliminary Milagro results for the inner Galaxy; in this

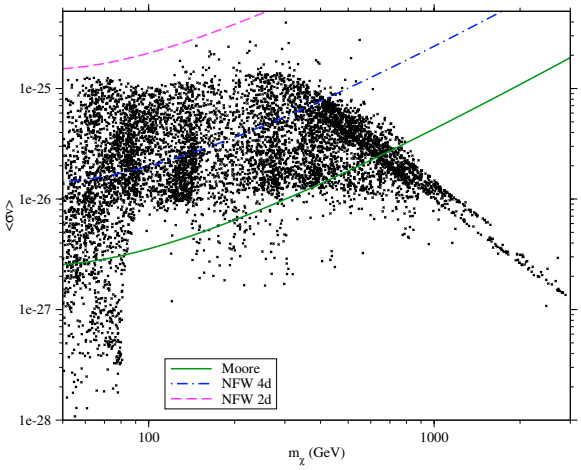

Fig. 4. The minimum detectable $\langle\sigma v\rangle$ (cm^3 s^{-1}) versus m_χ for Moore et al. profile and NFW (D&B 4d), NFW (D&B 2d) profiles. Dots: allowed SUSY models. Curves: 5σ detection level for ε (3 yr) = 216 cm^2 yr, $E_{\rm th}$ = 8 GeV, $\Delta\Omega$ = 1 msr around the Galactic Center. Only SUSY models that lie above the corresponding curve yield a detectable signal. A colour version of this plot is available on-line.

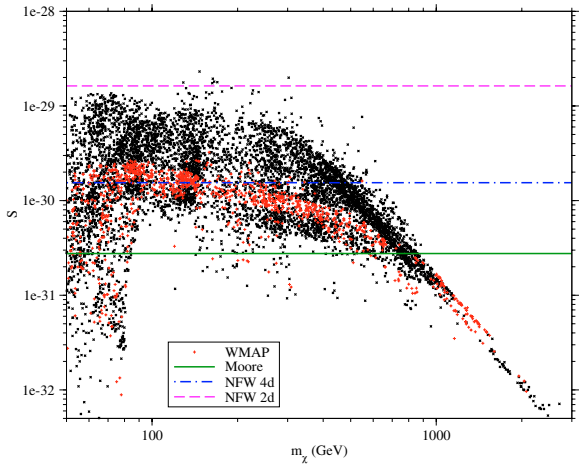

Fig. 5. The S factor (cm^3 s^{-1} GeV^{-2}) versus m_χ for Moore et al. profile and NFW (D&B 4d), NFW (D&B 2d) profiles. Dots: allowed SUSY models. Red dots: SUSY models satisfying WMAP cosmological constraint $0.094 < \Omega_\chi h^2 < 0.129$. Lines: 5σ detection level for ε (3 yr) = 216 cm^2 yr, $E_{\rm th}$ = 8 GeV, $\Delta\Omega$ = 1 msr around the Galactic Center. Only SUSY models that lie above the corresponding line yield a detectable signal. A colour version of this plot is available on-line.

Table 2. The ranges of parameters values used in the scans of SUSY parameter space.

μ	M_2	$\tan\beta$	m_A	m_0	$A_{\rm b}/m_0$	$A_{\rm t}/m_0$
GeV	GeV	1	GeV	GeV	1	1
–50 000	–50 000	3.0	0	100	–3	–3
+50 000	+50 000	60.0	10 000	30 000	+3	+3

region a differential spectral index of 2.63 ± 0.08 and an integral flux $F(>1\ \text{TeV}) = (8.0 \pm 3.3) \times 10^{-10}$ cm^{-1} sr^{-1} s^{-1} are obtained (Fleysher 2003).

6. The gamma continuum

We work in the frame of Minimal Supersymmetric extension of the Standard Model (MSSM). The MSSM has more than a hundred free parameters, but it is a common recipe to introduce some simplifying assumptions that leave only 7 parameters: the higgsino mass parameter μ, the gaugino mass parameter M_2, the ratio of the Higgs vacuum expectation values $\tan\beta$, the mass of the CP-odd Higgs boson m_A, the scalar mass parameter m_0, and the trilinear soft SUSY-breaking parameters $A_{\rm t}$ and $A_{\rm b}$ for the third generation quarks (for more details see, for instance, Bergstrom et al. 2001).

Using the computer code *DarkSUSY* (Gondolo et al. 2002), the parameter space has been sampled and Fig. 4 gives an idea of the wide boundaries of the allowed SUSY parameters. The limits for the seven MSSM parameters given in Table 2 (Tasitsiomi & Olinto 2002) were assumed. Each model plotted in Fig. 4 and in the following figures has been checked to see if it is excluded by the constraints due to measurements at accelerators, in particular by LEP bounds. For each model consistent with the accelerator constraints, the neutralino relic density $\Omega_\chi h^2$ has been calculated by the code (Edsjo & Gondolo 1997). Basing on cosmological constraints, the range $0.025 < \Omega_\chi h^2 < 0.2$ is adopted. The lower limit in the inequality is chosen by requiring that neutralinos are at least as abundant as necessary to make the dark halos of galaxies, even if this is somewhat arbitrary since there may be several different components of non-baryonic contributors to dark matter. The upper bound is chosen by taking into account the recent SN Ia observation (Riess et al. 1998; Perlmutter et al. 1999). About 8000 models satisfying all the above constraints have been plotted in Fig. 4.

This analysis is based on 25 random samples over the parameter space. Some of them are broad samplings in the parameters, others use more specific portions of the parameter space. The structures that can be seen in Figs. 4 and 5 and following, are mainly caused by the way the supersymmetric parameter space has been sampled.

The minimum detectable γ-ray flux is fixed here at the 5σ level:

$$\frac{N_{\rm S}}{\sqrt{N_{\rm B}}} \geq 5, \tag{13}$$

where $N_{\rm S}$ are the signal counts of a detector and $N_{\rm B}$ the background counts.Using this criterion we can constrain the SUSY parameter space. In Figs. 4 and 5 – in addition to the unknown neutralino parameters, $\langle\sigma v\rangle$ and m_χ – we consider the profile uncertainties by using the three density profiles NFW (D&B 2d), NFW (D&B 4d) and Moore et al. in Table 1. In these plots, the constraints on the neutralino parameter space are set as follows. The background counts are:

$$N_{\rm B}(E \geq E_{\rm th}) = \left[\int_{\Delta\Omega} \frac{{\rm d}N_{\rm B}}{{\rm d}\Omega}\ (E \geq E_{\rm th})\ {\rm d}\Omega\right]\varepsilon, \tag{14}$$

where $\frac{{\rm d}N_B}{{\rm d}\Omega}$ is given, in the case of irreducible γ background, by the expressions in Eqs. (12) and (11) integrated above the energy threshold of the detector, and $\Delta\Omega$ and ε (cm^2 yr) are, respectively, the angular resolution and the exposure (aperture

and orientation weighted time on source) of the detector. The signal counts N_S are given by

$$N_s = F_\gamma(\xi; \Delta\Omega)\, \varepsilon. \tag{15}$$

Equation (15) contains the yield N_γ, i.e. the number of γ-rays emitted per annihilation (Eq. (3)).

Substituting Eq. (15) for N_S and Eq. (14) for N_B in Eq. (13) and solving the resulting inequality with respect to $\langle\sigma v\rangle$, we obtain:

$$\langle\sigma v\rangle \geq f\left(J, \varepsilon, E_{\rm th}, \frac{dN_B}{d\Omega}, \Delta\Omega, n\right) m_\chi^2/N_\gamma(m_\chi). \tag{16}$$

Given a set of $\varepsilon, E_{\rm th}, \frac{dN_B}{d\Omega}, \Delta\Omega$, the detection level is obtained when $\langle\sigma v\rangle$ is greater than a value depending on m_χ and $J(\xi)$. The condition in Eq. (16) is drawn in Fig. 4, where we assume $\varepsilon(3\ \text{yr}) = 216\ \text{cm}^2\,\text{yr}$, $E_{\rm th} = 8$ GeV, $\Delta\Omega = 1$ msr around the Galactic Center. This set of values is referred to the features of the orbital experiment AMS-02, described in Sect. 8, but the procedure can be easily adapted for a different apparatus (both orbital and ground based experiments).

The parameter space divides into two regions: the one that can be detected according to Eq. (16) is above the line. Note that for the Moore et al. profile the region of parameter space that can be explored is quite wide, for the NFW 4d profile the allowed space is reduced by a factor of ≈5 and for the NFW 2d profile the situation is even worse. Lowering the threshold energy, increases N_γ (Eq. (4)). From inequality Eq. (16), it follows that a wider region of SUSY parameter space can be explored.

In Fig. 4, the values of N_γ used to draw the exclusion curves are calculated from Eq. (4), which takes into account only the mass of neutralino and not its state (the gaugino/higgsino percentages). A more accurate exclusion plot can be obtained considering the quantity S defined in Eq. (6); instead of inequality Eq. (16) we obtain:

$$S \geq f\left(J, \varepsilon, E_{\rm th}, \frac{dN_B}{d\Omega}, \Delta\Omega, n\right). \tag{17}$$

For the SUSY models plotted in Fig. 4, the corresponding S factors are shown in Fig. 5. These S values, that include the calculation of N_γ (see Eq. (6)), are computed using *DarkSUSY*, that takes into account the state of the neutralino. The horizontal lines of Fig. 5 arise using Moore et al. and NFW (D&B 4d), NFW (D&B 2d) profiles. In Fig. 5 the red dots represent the models (about 1000 among the 8000 calculated) satisfying the cosmological constraints from WMAP. The WMAP first year data (Bennett et al. 2003; Spergel et al. 2003) confirm with great accuracy the standard cosmological model and constrain the density of cold dark matter to the range $0.094 < \Omega_\chi h^2 < 0.129$, a range consistent with that inferred from earlier observations of MAXIMA-1, Boomerang and DASI (Lee et al. 2001; Netterfield et al. 2002; Pryke et al. 2002). From Fig. 5 we can note that the WMAP cosmological constraints define an almost horizontal strip for a wide range of masses, from $m_\chi \simeq 100$ GeV until to $m_\chi \simeq 600$ GeV. The selection of this restricted zone leaves almost unaltered the detection possibilities of neutralino dark matter particles if they are distributed following a Moore et al. profile. Instead the situation worsens considering the NFW 4d profile that, at the fixed 5σ detection level, allows the investigation of neutralinos with masses $m_\chi \lesssim 300$ GeV. Finally, if neutralino dark matter particles follows a NFW 2d profile, there is no hope detecting them with AMS-02 or similar instruments.

7. The gamma line channel

To investigate the detection efficiency for the line channel signature, the expected γ-ray counts in the operation time of the detector as a function of the solid angle Ω must be computed for any dark matter halo profile (see Eq. (15)). Given a detector resolution, an acceptance window corresponding to the required detection level and centered on the neutralino mass m_χ has to be considered. In this energy window the irreducible Galactic (Eq. (12)) and extragalactic (Eq. (11)) γ backgrounds must be calculated. The galactic background under the signal line at $E_0 = m_\chi$, i.e. in the range $[E_0 - \Delta E, E_0 + \Delta E]$, is given by integrating Eqs. (12):

$$N_0^{\rm int} = \int_{\Delta\Omega} N_0(l, b)\, d\Omega,$$

$$N_{\rm bg} = \frac{N_0^{\rm int}}{\alpha - 1} E_0^{1-\alpha} \eta(\Delta E/E, \alpha)\ \ \text{cm}^{-2}\,\text{s}^{-1}, \tag{18}$$

where:

$$\eta(\Delta E/E, \alpha) = \left[(1 - \Delta E/E)^{1-\alpha} - (1 + \Delta E/E)^{1-\alpha}\right].$$

An application of this criterion is given in Sect. 8.3 for the orbital experiment AMS-02.

8. Detection prediction for an orbital experiment

As an example of an orbital experiment, we examine the detection prediction in the case of the Alpha Magnetic Spectrometer (AMS, Alpat 2001), an assembly of several detectors among which is an electromagnetic calorimeter. It will be installed on International Space Station (ISS) for a period of 3 years, operating in a range of energies from few GeV–1 TeV. It can investigate local DM evidence; among its goals is the search for an indirect signature of neutralino via the gamma ray channels. This experiment is able to detect photons with two complementary methods: the *single photon mode* and the *conversion mode*. The *single photon mode* consists of the detection of photons that impinge on the electromagnetic calorimeter without interacting with the other detectors; the calorimeter, equipped with a stand-alone trigger, can be used to identify and measure these photons. The *conversion mode* consists in the identification and reconstruction of e^+e^- pairs originating from γ–conversion in the material upstream from the first silicon tracker layer. This analysis is performed for photons arriving without conversion on the calorimeter surface: they amount to about 70% of total number of photons impinging on the AMS-02. A more extensive analysis can be found in Valle (2003).

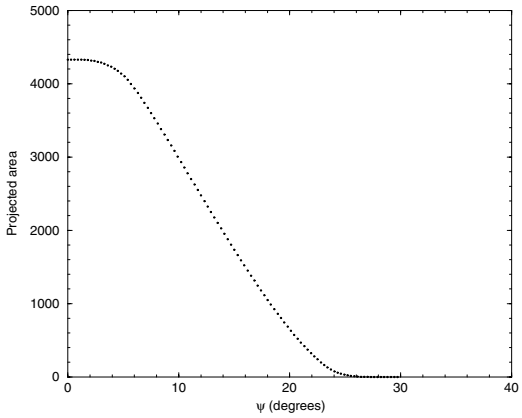

Fig. 6. Expected projected area $A(\psi)$ (cm^2) as a function of ψ.

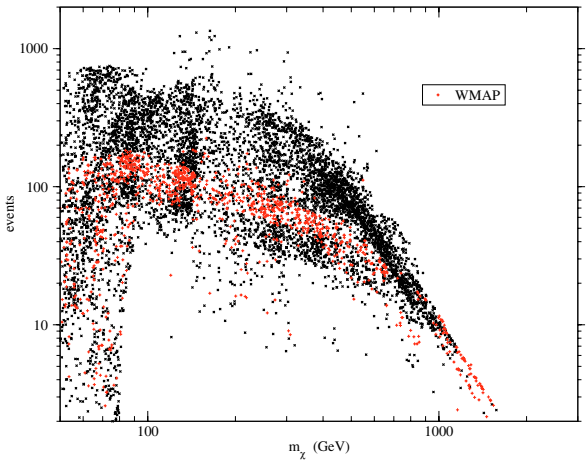

Fig. 8. The number of events detectable for AMS-02 in single photon mode in 3 yr, for $\Delta\Omega = 1$ msr around the Galactic Center, ε (3 yr) = 216 cm^2 yr, $E_{\rm th} = 8$ GeV, for the Moore et al. profile, as a function of neutralino mass for the SUSY models plotted also in Fig. 5 The red dots are the models satisfying WMAP cosmological constraint $0.094 < \Omega_\chi h^2 < 0.129$. A colour version of this plot is available on-line.

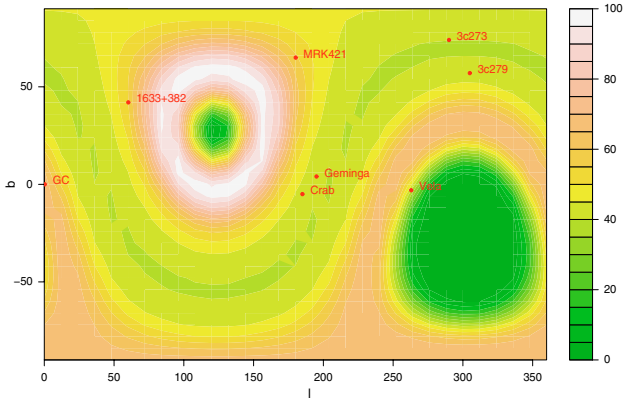

Fig. 7. AMS-02 exposure ε (cm^2 yr) with some γ sources as a function of galactic coordinates b (latitude) and l (longitude), for 1 yr. A colour version of this plot is available on-line.

8.1. Instrumental exposure

AMS-02 is not a pointing instrument: it will be rigidly attached to the ISS. It will not spend equal amounts of time viewing all directions in the celestial sphere. Full sky coverage is obtained approximately every 70 days due to ISS orbital precession.

How much time is spent by AMS-02 observing a celestial source in its detection cone and how the angle varies between the AMS-02 zenith and the source is characterized by the exposure function ε (cm^2 yr) used in Figs. 4 and 5. The number of events expected in any time interval can be calculated from Eq. (15). The geometry of the apparatus is computed separately; we obtain the dependence of the illuminated calorimeter area as a function of the photon incidence angle between the zenith of AMS-02 and the source direction ψ. The result is shown in Fig. 6: the illuminated area vanishes at about 28°. To obtain an estimate of the expected events, the geometrical information shown in Fig. 6 is combined with the orbital motion, using an orbital simulation code which gives the position pointed by AMS-02 as a function of time to find the ε function (Valle 2003). The resulting exposure ε, as a function of the Galactic coordinates b and l is shown in Fig. 7, which also shows the positions of some important γ sources (Crab, Vela, Geminga, MRK 421, 3C 273, 3C 279, 1633+382) that AMS-02 can observe during its period of operation. We note that the Galactic Center, the region in which the assumed dark matter halo profiles are enhanced, corresponds to high exposure.

8.2. Numerical results for the gamma continuum

Figure 8 is obtained multiplying the values of the S factor plotted in Fig. 5 by the part depending only on astrophysical quantities, calculated for the Moore et al. profile (Eq. (10)) and by the exposure ε. From Fig. 8 it is possible to read the number of events from neutralino annihilation in the continuum, as a function of m_χ, that can be detected with AMS-02 in 3 yr in orbit in the single photon mode. The models satisfying the WMAP cosmological constraint are represented with red dots. The number of events for the NFW D&B 4d and NFW D&B 2d profiles can be obtained with a scaling of the factor $J(\xi;\Delta\Omega)$ (see Fig. 2). The same procedure holds for $S_{\rm p}$, $K_{\rm b}$ profiles (see Fig. 3).

The choice of $\Delta\Omega = 1$ msr as solid angle of integration (compatible with the detector angular resolution) instead of the entire field of view has been adopted to enhance the signal to noise ratio. In fact, in the energy range of interest, the γ background is dominated by the Galactic component, which is not uniform but concentrated around the Galactic Center. Nevertheless, at least for the dark matter distributions analyzed, the neutralino signal is more concentrated around the Galactic Center than the γ background; so, selecting a smaller $\Delta\Omega$, the signal to noise ratio increases.

Moreover, to assess the capability to detect a neutralino signature, the important cosmic ray (CR) background which mimics a photon signal in the experimental apparatus, must to be taken into account. The main CR component is protons (the ratio between protons and γ at energy of about 10 GeV is 10^4–10^5), followed by He and C nuclei and electrons. Given the high rejection capability of the instrument (Maestro 2003) and selecting the solid angle of $\Delta\Omega = 1$ msr around the Galactic

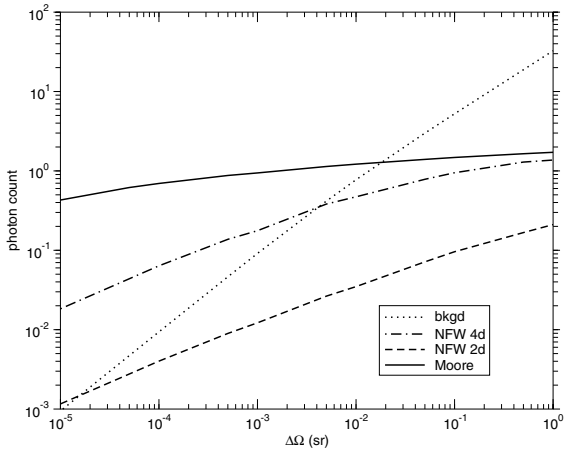

Fig. 9. Integrated photon counts vs. $\Delta\Omega$ for the annihilation γ line integrated over 3 years for NFW (D&B 2d), NFW (D&B 4d) and Moore et al. profiles for $m_\chi = 78$ GeV.

Center, the protons counts can be reduced to a negligible level (Valle 2003). As a final remark, in the previous events calculations, AMS-02 was treated as an ideal instrument, neglecting the loss of events due to the reconstruction efficiency and trigger efficiency. However, this loss of events is estimated to be only a few percent in the case of looking toward the Galactic Center.

8.3. Numerical results for the gamma line channel

To investigate the AMS-02 detection efficiency for the γ line, the integrated γ-ray counts in 3 yr as a function of the solid angle Ω around the Galactic Center were calculated for the first three dark matter halo profiles listed in Table 1. In order to get a scenario with the potential highest fluxes, we consider a MSSM model $\chi\chi \rightarrow \gamma\gamma$ at $m_\chi = 78$ GeV, giving $S_{\max} \simeq 7.6 \times 10^{-33}$ cm^3 s^{-1} GeV^{-2} (Bergstrom et al. 2001).

The calorimeter energy resolution (Cervelli et al. 2002) $\sigma(E)/E \simeq 2.5\%$ at 78 GeV, an acceptance window of $2\Delta E = 12$ GeV, corresponding to a 3σ level, and centered on the neutralino mass have been considered.

The results are shown in Fig. 9 for NFW (D&B 4d), NFW (D&B 2d) and Moore et al. profiles. The integrated number of events as a function of the solid angle Ω around the Galactic Center is <1 for halo dark matter profiles NFW (D&B 4d), NFW (D&B 2d) and smaller than the γ-background for NFW (D&B 2d); the Moore et al. profile produces an integrated number of events $\simeq$1. For the Moore et al. profile, enlarging the solid angle of integration, the number of photon counts doesn't change appreciably and is almost constant for solid angles greater than $\Delta\Omega = 1$ msr. This behaviour is due to the steeper radial dependence of Moore et al. profile relative to NFW 2d, 4d profiles. As in the case of the continuum, to maximize the signal to noise ratio, it is convenient to integrate over a small solid angle of order $\Omega \simeq 1$ msr around the Galactic Center, which contains most of the halo dark matter density profile. Still the number of counts is negligible and the line signature cannot be detected by AMS-02 under our assumptions. It might be possible to detect such a signature with dark matter models that have stronger cusps or clumps than those investigated in this work.

9. Comparison with ground based detectors

In this paper we proposed as an example the γ line and continuum detection possibilities of the orbital experiment AMS-02. As underlined before, the exposed procedure is general and allows us to make predictions regarding other experiments, orbital or not, for which the main characteristics are known. An interesting comparison can be made between an orbital instrument and a ground based one, like an Imaging Atmospheric Cerenkov Telescope (IACT). With respect to an orbital experiment, IACTs are usually characterized by larger effective area which increases the signal counts, and higher threshold in energy which produces the opposite effect.

A reasonable set of parameters for the present IACTs (HESS, MAGIC, VERITAS, CANGAROO-III, etc.) are: angular resolution $\sigma = 0.1^\circ$, solid angle $\Delta\Omega = 10^{-5}$ sr, threshold energy $E_{\rm th} = 100$ GeV, effective area $A_{\rm eff} \simeq 10^8$–10^9 cm^2, exposure time of $t \simeq 100$–200 hours (Tasitsiomi and Olinto 2002; Prada et al. 2002). We assume here $A_{\rm eff} = 10^9$ cm^2, $t = 200$ h.

Let $N_{\rm AMS}$ and $N_{\rm IACT}$ be, respectively, the signal counts (Eq. (15)) expected for AMS and for a generic IACT. We derive the following scaling law:

$$\frac{N_{\rm AMS}}{N_{\rm IACT}} = \frac{(A_{\rm eff}\, t)_{\rm IACT}}{\varepsilon_{\rm AMS}} \frac{N_{\gamma\,\rm IACT}}{N_{\gamma\,\rm AMS}} \frac{J(\xi;\Delta\Omega_{\rm AMS})}{J(\xi;\Delta\Omega_{\rm IACT})}. \tag{19}$$

To make a rough comparison between the detection capabilities of these two instruments, we must also evaluate the main IACT hadronic and electronic background sources, due to the cosmic ray showers. Adopting for the hadronic background the expression given in Bergstrom et al. (1998), derived from Whipple telescope data, and for the electron background that given in Longair (1992), the backgrounds counts are given by:

$$N_h(E > E_{\rm th}) = 6.1 \times 10^{-3} \left(\frac{E_{\rm th}}{1\ \rm GeV}\right)^{-1.7} A_{\rm eff}\ t\ \Delta\Omega, \tag{20}$$

$$N_{\rm e^-}(E > E_{\rm th}) = 3.0 \times 10^{-2} \left(\frac{E_{\rm th}}{1\ \rm GeV}\right)^{-2.3} A_{\rm eff}\ t\ \Delta\Omega. \tag{21}$$

In the continuum case, the Moore profile shows AMS outperforming the ground based experiments for light neutralino masses up to $m_\chi \lesssim 150$ GeV, while for high masses the opposite trend results. The IACTs detection threshold $E_{\rm th}$ and effective area $A_{\rm eff}$ depend also on the zenith angle of observation, so the Galactic Center region is not equally favored for DM searches for the different Cerenkov telescopes at different zenith angle. However, from the analysis performed here we can conclude that IACTs have a complementary role with respect to γ-ray satellites, allowing a more sensitive investigation on larger neutralino masses.

Acknowledgements. I wish to thank deeply Steve Shore for many valuable discussions and advice on this paper. I also thank the referee, Dr. S. D. Hunter, for his critical reading and helpful suggestions.

References

Alpat, B. 2001, Nucl. Inst. Meth. A, 461, 272

Bennett, C. L., Halpern, M., Hinshaw, G., et al. 2003, ApJS, 148, 1

Bergstrom, L., Edsjo, J., & Gunnarsson, C. 2001, Phys. Rev. D, 63, 083515

Bergstrom, L., Ullio, P., & Buckley, J. H. 1998, Astropart. Phys., 9, 137

Calcaneo-Roldan, C., & Moore, B. W. 2000, Phys. Rev. D, 62, 123005

Cervelli, F., Di Falco, S., Lomtadze., T., et al. 2002, Performances of the AMS-02 Electromagnetic Calorimeter. In 10th International Conference on Calorimetry in High Energy Physics (CALOR 2002), Pasadena 2002, Calorimetry in particle physics, 114

Dehnen, W., & Binney, J. 1998, MNRAS, 294, 429

Edsjo, J., & Gondolo, P. 1997, Phys. Rev. D, 56, 1879

Ellis, J. 1999, Particles and Cosmology: Learning from Cosmic Rays, Proc. 26th International Cosmic-Ray Conf., Salt Lake City, August 1999 [arXiv:astro-ph/9911440]

Fleysher, R. 2003, for Milagro Collaboration, 28th International Cosmic-Ray Conf., 2269

Fukushige, T., & Makino, J. 2000, Constructing the Universe with Clusters of Galaxies, IAP 2000 Meet., Paris, France, July 2000, ed. Durret, & Gerbal

Gondolo, P., Edsjo, J., Ullio, P., et al. 2002, Proc. 4th International Workshop on Identification of Dark Matter (idm2002), York, England, 2–6 September [arXiv:astro-ph/0211238]

Hagiwara, K., Hikasa, K., Nakamura, K., et al. 2002, Phys. Rev. D, 66, 010001

Hunter, S. D., Bertsch, D. L., Catelli, J. R., et al. 1997, ApJ, 481, 205

Jing, Y. P., & Suto, Y. 2000, ApJ, 529, L69

Jungman, G., Kamionkowski, M., & Griest, K. 1996, Phys. Rep., 267, 195

Kravtsov, A. V., Klypin, A. A., Bullock, J. S., & Primack, J. R. 1998, ApJ, 502, 48

Lee, A. T., Ade, P., Balbi, A., et al. 2001, ApJ, 561, L1

Longair, M. S. 1992, High Energy Astrophysics (Cambridge, England: Cambridge University Press)

Maestro, P. 2003, Ph.D. Thesis, University of Siena, http://www.pi.infn.it/~maestro/

Moore, B., Quinn, T., Governato, F., et al. 1999, MNRAS, 310, 1147

Navarro, J. F., Frenk, C. S., & White, S. D. M. 1996, ApJ, 462, 563

Netterfield, C. B., Ade, P. A. R., Bock, J. J., et al. 2002, ApJ, 571, 604

Perlmutter, S., Aldering, G., Goldhaber, G., et al. 1999, ApJ, 517, 565

Prada, F., Klypin, A., Flix, J., et al. 2004 [arXiv:astro-ph/0401512]

Press, W. H., & Farrar, G. R. 1990, Computers in Physics, 2, 190

Pryke, C., Halverson, N. W., Leitch, E. M., et al. 2002, ApJ, 568, 46

Riess, A. G., Filippenko, A. V., Challis, P., et al. 1998, AJ, 116, 1009

Schoedel, R., Genzel, R., Baganoff, F. K., & Eckart, A. 2004, Galactic Center Newsletter, ed. Markoff, Sjouwerman, Lazio, Lang, & Schoedel, 17, 5

Spergel, D. N., Verde, L., Peiris, H. V., et al. 2003, ApJS, 148, 175

Sreekumar, P., Bertsch, D. L., Dingus, B. L., et al. 1998, ApJ, 494, 523

Steinmetz, M., & Navarro, J. F. 2002, New Astron., 7(4), 155

Tasitsiomi, A., & Olinto, A. V. 2002, Phys. Rev. D, 66, 083006

Valle, G. 2003, Ph.D. Thesis, Dark Matter Search in the gamma channel with the AMS-02 Experiment University of Siena, http://www.pi.infn.it/~valle/

Zhao, H. S. 1996, MNRAS, 278, 488